Charge density analysis of SiO_2 under pressures over 50 GPa using a new diamond anvil cell for single-crystal structure analysis

2002 J. Phys.: Condens. Matter 14 10545

(http://iopscience.iop.org/0953-8984/14/44/330)

INSTITUTE OF PHYSICS PUBLISHING JOURNAL OF PHYSICS: CONDENSED MATTER

J. Phys.: Condens. Matter **14** (2002) 10545–10551 PII: S0953-8984(02)38476-5

Charge density analysis of SiO_2 under pressures over 50 GPa using a new diamond anvil cell for single-crystal structure analysis

T Yamanaka[1], **T Fukuda**[1], **Y Komatsu**[1] **and H Sumiya**[2]

[1] Department of Earth and Space Science, Osaka University, Toyonaka, Osaka 560-0043, Japan
[2] Itami Research Laboratories, Sumitomo Electric Industries, Ltd, Koya-kita Itami, Hyogo 664-0016, Japan

Received 19 June 2002
Published 25 October 2002
Online at stacks.iop.org/JPhysCM/14/10545

Abstract

Single-crystal structure analysis of SiO_2 stishovite, (rutile type, $P4_2/mnm$ $z = 2$) was carried out using the newly devised diamond anvil cell. The electron-density distribution was investigated at high pressures up to 50 GPa using synchrotron radiation at SPring-8 and a laboratory x-ray source generator of Ag Kα rotating anode generator. Using large diamond crystal windows instead of beryllium for the cell has several advantages for single-crystal diffraction study supplying the large Q-value.

1. Introduction

Stishovite is (rutile type, $P4_2/mnm$ $Z = 2$) one of the high-pressure polymorphs of SiO_2 and has a rutile type structure. It is one of the major lower-mantle materials and stabilized over 10 GPa. The bulk modulus and structure transitions of the material have been investigated by geophysicists under compression.

The single-crystal structure analysis of SiO_2 stishovite was first described by Sinclair and Ringwood [1]. The electron-density distribution of SiO_2 has been investigated at ambient pressure using x-ray diffraction study [2–4]. The crystal structure analyses under pressures up to 6 GPa [5] and 16 GPa [6] have been reported.

A molecular orbital calculation makes a precise discussion of the density of electronic states of bond nature. The bonding electron observed from the x-ray diffraction study was interpreted by a molecular orbital calculation [7, 8]. The electron orbital overlap causes the deformation of SiO_6 octahedra of stishovite structure [9–11]. However, the electron density distribution under compression has never been examined by experiment, because of the poor resolution of Fourier analysis based on x-ray diffraction intensities. The density distribution of crystals under high-pressure conditions has been devoted a large amount of interest in order to understand the pressure-induced transformation. The coulomb potential and interatomic force must be affected by the stress field. We carried out the single-crystal structure analysis

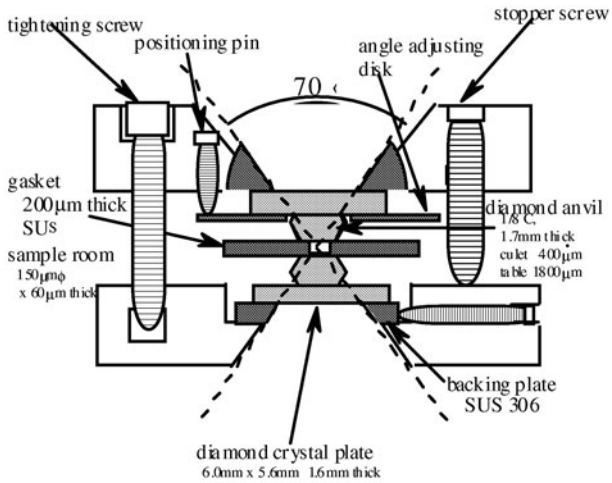

Figure 1. DAC with diamond crystal window.

of SiO_2 stishovite, using the newly devised diamond anvil cell (DAC). The electron-density distribution of SiO_2 has been investigated at high pressures up to 50 GPa.

2. New diamond anvil cell

A new DAC was devised for the single-crystal structure analyses under high pressure. The cell is characterized by large single-crystal diamond window plates (Ib diamond of 6 mm × 6 mm wide and 2 mm thick about 2 carats) set on the table planes of diamond anvils.

The DAC cross section is shown in figure 1. Liquid argon was used as the transmitting media in order to preserve the hydrostatic conditions. The wavelength of $E = 30.388$ keV emitted from the bending magnet of SR source with 8 GeV 100 mA at SPring-8 was used for the diffraction intensity measurement. The short wavelength through the diamond window allowed one to observe reflections up to $d > 0.44150$ Å. The number of observed reflections is four times more than those obtained from the laboratory source of Mo Kα and Ag Kα. The new assembly solves many problems in high-pressure diffraction measurement and it greatly improves the accuracy of the structure analysis. Diamond plate windows have the following advantages for single-crystal diffractometry:

(1) low x-ray absorption from the window;
(2) much higher pressure observation than the beryllium plate;
(3) no powder ring from the window;
(4) wide opening 2θ-angle ($2\theta < 70°$);
(5) transparent window advantage for sample setting.

These advantages could measure the intensities of much high order reflections and the precise electron density distribution was discussed as a function of pressure. The more detailed specification of the new DAC was reported in [12].

3. Structure analysis

The lattice constants under pressure were determined on the basis of the diffraction angle of 15–25 reflections with $20° < 2\theta < 30°$. V/V_0 change of SiO_2 stishovite with pressure is plotted

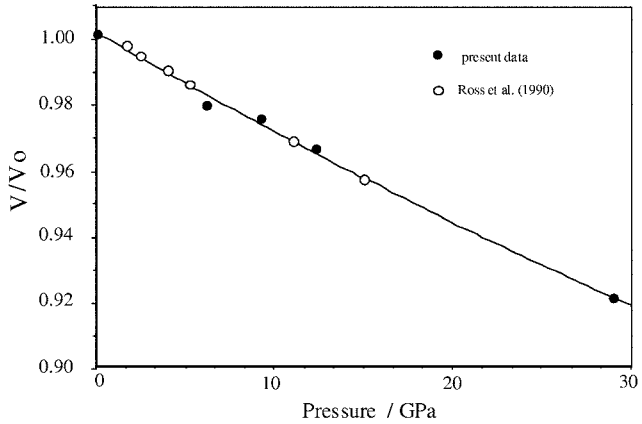

Figure 2. V/V_0 change of SiO_2 stishovite with pressure. Present data are plotted by full circles and the data represented by the open circles are from Ross *et al* [6].

Table 1. Conditions of intensity measurements.

Pressure (GPa)	Ambient	5.23	9.26	12.3	29.1
Four circle	RIGAKU AFC5s	RIGAKU AFC6R			SPring-8
Wavelength	Mo Kα (0.7107ð)	Ag Kα (0.5608ð)			SR (0.4077ð)
Energy	150 kV 50 mA	150 kV 50 mA			8 GeV 100 mA
Monochrometer	Graphite (002)	Graphite (002)			Si (111) double
Gasket		Spring steel			Spring steel
Pressure media		$M:E:W = 16{:}3{:}1$			Ar
Scan mode	$\omega - 2\theta$	ϕ-fix mode			ω-scan
Crystal size (μm)	$50 \times 60 \times 80$	$40 \times 40 \times 60$			$20 \times 20 \times 40$
2θ angle	120	53	47	54	49
$\sin\theta/\lambda$	1.219	0.794	0.714	0.801	1.011
2θ angle(Mo Kα)	120	69	61	70	92
Ref. (independent)	126	25	25	26	31

in figure 2. The isothermal bulk modulus (K_0) was calculated from the volume change using the Birch–Murghnan equation. The large K_0 (=252(13) GPa) and $\mathrm{d}K/\mathrm{d}P = 4.3$ indicates that SiO_2 stishovite is a noticeably hard crystal.

The conditions of diffraction intensity measurements at 0.0001, 5.23, 9.26, 12.3 and 29.1 GPa are listed in table 1. For the structure refinement under compression, diffraction intensities were measured by the ϕ-fixed and, ω-scan mode, with a scan speed of 0.5° or 1° min, a scan width of 2° in ω and step interval 0.01° /step. Reflections up to $hkl = 661$ with $d = 0.4679$ Å at $2\theta = 51.7°$ were observed, 147 reflections were observed at 29.1 GPa and among them 31 and 47 independent reflections for $F_0 > 3\sigma(F_0)$ and $F_0 > 2\sigma(F_0)$ were used for the structure refinement.

The structure analysis at each pressure was carried out using full matrix least-squares refinement. The conventional least-squares refinement was first executed including the variable isotropic extinction parameter G_{ex}. Anharmonic thermal vibration of atoms is negligibly small at room temperature, because the SiO_2 sample has quite a high Debye temperature. Consequently, higher rank thermal parameters rather than second ranks derived from a harmonic model were not applied in the refinement.

After the refinement, the charge density was elucidated by monopole refinement in the least-squares optimization using the structure factor $F(hkl)$ [13].

The inner core electrons are assumed to be 'frozen' and regardless of the perturbations associated with bonding effects by the pseudopotential model. The valence electrons are not bound tightly to the nuclei and their interactions with the core electrons are relatively weak. Accordingly they are more sensitive to the coordination of the adjacent atoms and characterized by non-spherical distributions. The deformation electron densities have been analyzed by the monopole refinement. The κ-parameter is an indicator of the radial distributions of the electrons. A localized electron distribution implies more ionicity in the chemical bond. The atomic scattering factor $f(s)$ of structure refinement is modified from a Hartree–Fock approximation based on the isolated atom model. The perturbed valence density is given by

$$\rho'_{valence}(r) = P_{valence} \cdot \kappa^3 \cdot \rho_{valence}(\kappa \cdot r), \tag{1}$$

where $\rho_{valence}(r)$ is the ground state density of the free atom, $P_{valence}$ is the valence-shell population, which is assigned to the occupancy parameter of core and valence electrons, and the factor κ^3 is required for normalization. The following atomic scattering factor is used for the present structure refinement:

$$f(s/2) = f_{j,core}(s/2) + P_{j,valence} f_{j,M-core}(\kappa_j, s/2) + f'_j + \mathrm{i} f''_j. \tag{2}$$

The valence scattering of the perturbed atom at $s/2$ ($= \sin\theta/2\lambda$) is given by

$$f_{M-core}(\kappa_j, s/2) = f_{j,M-core(free\,atom)}(\sin\theta/\lambda \cdot 1/\kappa_j). \tag{3}$$

Consequently the valence charge of the cation was accounted for only population parameter. The P and κ parameters could be simultaneously refined with all the other parameters. The valence electrons around the atomic position and the bonding electron distribution cannot be separately evaluated by structure refinement. The difference Fourier synthesis and the population parameter show an electron deformation density. The effective charge q is obtained by the spatial integration of the difference electron density by

$$q = -\int \Delta\rho(r)\,\mathrm{d}r = -4\pi \int r^2 \cdot \rho(r)\,\mathrm{d}r. \tag{4}$$

Accordingly q has a correlation with the κ-parameter.

4. Result of monopole-refinement

The refined structure parameter data are shown in table 2. The converged structure parameters of SiO_2 are in good agreement with the previous experimental data [2–4]. Interatomic distances are presented in table 3. The population parameter P of the valence electrons in equation (2) defines the effective charge of the oxygen atoms. The κ-parameters and oxygen valence electrons of SiO_2 at 0.0001 and 29.1 GPa are 0.94 and 1.11 respectively.

The population parameter was optimized together with the κ-parameter. In the refinement the charge was constrained to be neutral in the bulk crystal. The electron distributions on their Si–O bonds are more localized and more ionic with increasing pressure. More bonding electrons in the covalent-bonded structure indicate a smaller κ-parameter. After the refinement with the spherical-atom model, the deformations of the electron distributions of SiO_2 at the two pressures are disclosed by difference Fourier synthesis on the plane (110) as shown in figures 3(a) and (b). The map of SiO_2 shown in figure 3(a) is very similar to that of Spackman *et al* [3].

A positive peak with a height of 0.7 eV A^{-3} is found at almost the middle position of the Si–O bond at 0.0001 GPa. Four positive residual densities are also recognized at 0.4 Å from the Si position. The non-spherical residual electron density around Si is probably induced from overlapping orbitals resulting in d–p-π bond.

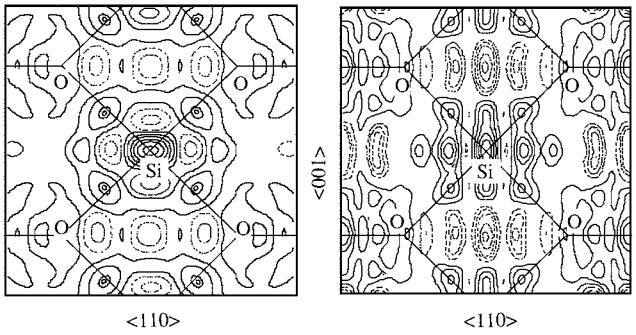

Figure 3. Residual electron distribution under ambient conditions and 29.1 GPa. Projection is onto (110). Contours are at intervals of 0.2 e/A^3 and positive and negative contours are expressed by the solid and broken lines, respectively. The deformation density of the valence electron is revealed around the cation and bonding electron distribution in the Si–O bond: (a) ambient condition; (b) 29.1 GPa.

Table 2. Converged structure parameter.

Pressure	1 atm	5.23 GPa	9.26 GPa	12.3 GPa	29.1 GPa
a(Å)	4.1812(1)	4.152(1)	4.134(1)	4.118(2)	4.044(6)
c(Å)	2.6662(3)	2.6590(8)	2.6540(7)	2.649(1)	2.619(2)
c/a	0.6366	0.6404	0.6420	0.6432	0.6492
V(Å^3)	46.533	45.639	45.396	44.922	42.524
No ref	126	25	25	26	36
$R(F)$	0.0253	0.0440	0.0312	0.0345	0.0330
$wR(F)$	0.0243	0.0234	0.0104	0.0227	0.0082
Si (000)					
b_{11}	0.0045(1)	0.0126(27)	0.0055(21)	0.0088(20)	0.0035(11)
b_{33}	0.0037(5)	0.0261(18)	0.0142(12)	0.0103(13)	0.0131(13)
b_{12}	0.0002(2)	0.0004(21)	0.0021(14)	0.0009(12)	0.0019(15)
O ($xx0$)	0.3063(1)	0.3063(20)	0.3056(9)	0.3058(19)	0.3039(7)
b_{11}	0.0051(2)	0.0075(37)	0.0051(29)	0.0104(21)	0.0095(13)
b_{33}	0.0036(3)	0.0164(17)	0.0031(28)	0.0090(18)	0.0104(17)
b_{12}	−0.0009(3)	0.0005(35)	0.0009(29)	0.0007(35)	0.0004(16)

Table 3. Interatomic distance of rutile-type SiO_2 (stishovite).

Pressure	1 atm	5.23 GPa	9.26 GPa	12.3 GPa	29.1 GPa
Si–O(eq) × 4	1.7559(9)	1.750(11)	1.748(8)	1.742(13)	1.724(19)
Si–O(ap) × 2	1.8111(9)	1.798(4)	1.784(2)	1.781(4)	1.738(7)
ap/eq	1.0314	1.0274	1.0194	1.0223	1.0055
O1–O2(sh)	2.2906(10)	2.277(5)	2.275(3)	2.262(5)	2.242(7)
O1–O1(unsh)	2.617(20)	2.6662(3)	2.659(8)	2.654(7)	2.649(1)
O1–O3	2.5226(4)	2.509(10)	2.498(10)	2.482(17)	2.448(25)
sh/unsh	0.8591	0.8563	0.8571	0.8539	0.8552

The noticeable electron density on the Si–O bond indicates a bonding electron. A large negative density in the bridging O–O bond plays a role of the hindrance of cation repulsion. This feature is caused by the difference in the covalency/iconicity ratio, which was explained from

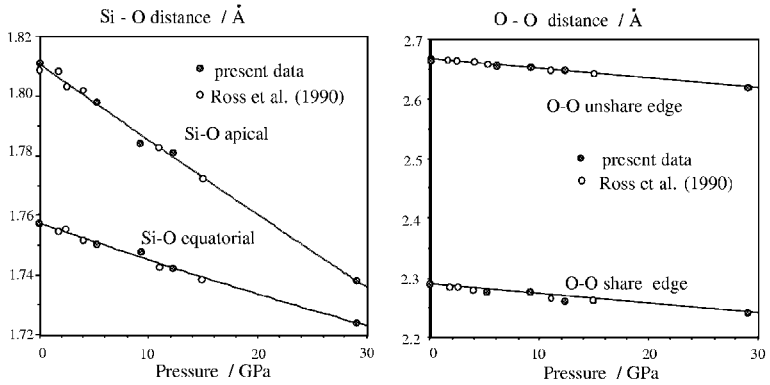

Figure 4. Interatomic distance change with pressure. Compression curves of both Si–O bonds are a little different from Ross *et al* [6].

the observed κ-parameter and effective charge. These data indicate that SiO_2 at 0.0001 GPa has a more covalent character than that of at 29.1 GPa and that the ionicity in the Si–O bond is more intensified with increasing pressure.

5. Discussion

The charge distribution reveals a significant admixture of covalency in the chemical bonds of rutile-type oxides and the appropriate charge state of the cations turns out to be far from a formal charge of Si^{4+} configuration. Our results are well consistent with an energy band calculation [9] and a cluster-model calculation [11]. The significant d-electron population indicates some degree of non-sphericity of the valence electron distribution around the cation. The difference Fourier synthesis (figure 3) reveals the apparent non-sphericity around Si.

The bonding electrons are related to the overlapped orbits of s and p electrons together with d electrons. In order to investigate the bond character of rutile-type structures we carried out the molecular orbital calculation.

The dipole moment (μ) may be experimentally determined by summation of product of charge (q) and interatomic distance (r):

$$\mu_{obs} = \Sigma q_i r_i \tag{5}$$

where q_i is the same value as the population P_i obtained from the present κ-refinement.

An apparent relative ionicity of SiO_2 at 0.0001 GPa can be expressed by μ_{obs}/μ_{ideal}, where μ_{ideal} is determined by the formal charge and interatomic distance. The result of the apparent relative ionicity of Si^{4+} is +2.12(8) for 0.0001 GPa and +2.26(15) for 29.1 GPa.

The electronic orbital overlapping causes the deformation of octahedral coordination SiO_6 of the rutile-type structures and the bond character about the covalency/ionicity. The d-electron of cations increases the degree of d–p-π bond in Si–O. The ratio between shared and unshared edge distance of O–O has a strong relation to the interatomic repulsive force between two cations Si–Si and the degree of π bond of Si–O. The shared/unshared parameter presented in table 3 indicates that the ratio decreases with increase in cation ionicity. The interatomic Si–O and O–O distances are plotted with the ratio c/a in figure 4. Si–O(apical) and Si–O(equatorial) become closer to each other, because the valence electron distribution in SiO_6 octahedra turns to be isotropic resulting in spherical under high pressure. Unusually the shorter shared O–O edge is more shrunken with compression than the unshared edge. Our previous powder

diffraction study found that stishovite transforms to the $CaCl_2$-type structure above 58 GPa. This transformation is along the process of the pressure effect on the valence electron discussed above.

References

[1] Sinclar W and Ringwood A E 1978 *Nature* **272** 714–15
[2] Hill R J, Newton M D and Gibbs G V 1983 *J. Solid State Chem.* **47** 185
[3] Spackman M A, Hill R J and Gibbs G V 1987 *Phys. Chem. Miner.* **14** 139
[4] Yamanaka T, Kurashima R and Mimaki J 2000 *Z. Kristallogr.* **215** 424
[5] Sugiyama M, Endo S and Koto K 1987 *Miner. J.* **13** 455
[6] Ross N L, Shu J F, Hazen R M and Gasparik T 1990 *Am. Miner.* **75** 739
[7] Svane A and Antoncik E 1987 *J. Phys. Chem. Solids.* **48** 171
[8] Mimaki J, Tsuchiya T and Yamanaka T 2000 *Z. Kristallogr.* **215** 419
[9] Simunek A, Vackar J and Wiech G 1993 *J. Phys.: Condens. Matter* **5** 867
[10] Camargo A C, Igualada J A, Beltràn A, Lhusar R, Longo E and Andres J 1996 *Chem. Phys.* **212** 381
[11] Gibbs G V, Hill F C and Boisen M B Jr 1997 *Phys. Chem. Min.* **24** 167
[12] Yamanaka T, Fukuda T, Hattori T and Sumiya H 2001 *Rev. Sci. Instrum.* **72** 1458
[13] Coppens P, Guru Row T N, Leung P, Stevens E D, Becker P J and Yang W 1979 *Acta Crystallogr.* A **35** 63